Supplement of Atmos. Chem. Phys., 21, 8323–8339, 2021
https://doi.org/10.5194/acp-21-8323-2021-supplement

Supplement of

Increase in secondary organic aerosol in an urban environment

Marta Via et al.

Correspondence to: Marta Via (marta.via@idaea.csic.es) and María Cruz Minguillón (mariacruz.minguillon@idaea.csic.es)

Supplementary material

Section 1. Supplementary tables and figures

Map data ©2021 Inst. Geogr. Nacional, Google, Institut Cartogràfic de Catalunya

Figure S 1. Location of Palau Reial and the Faculty of Physics in aerial view zoom to the site (Google Maps).

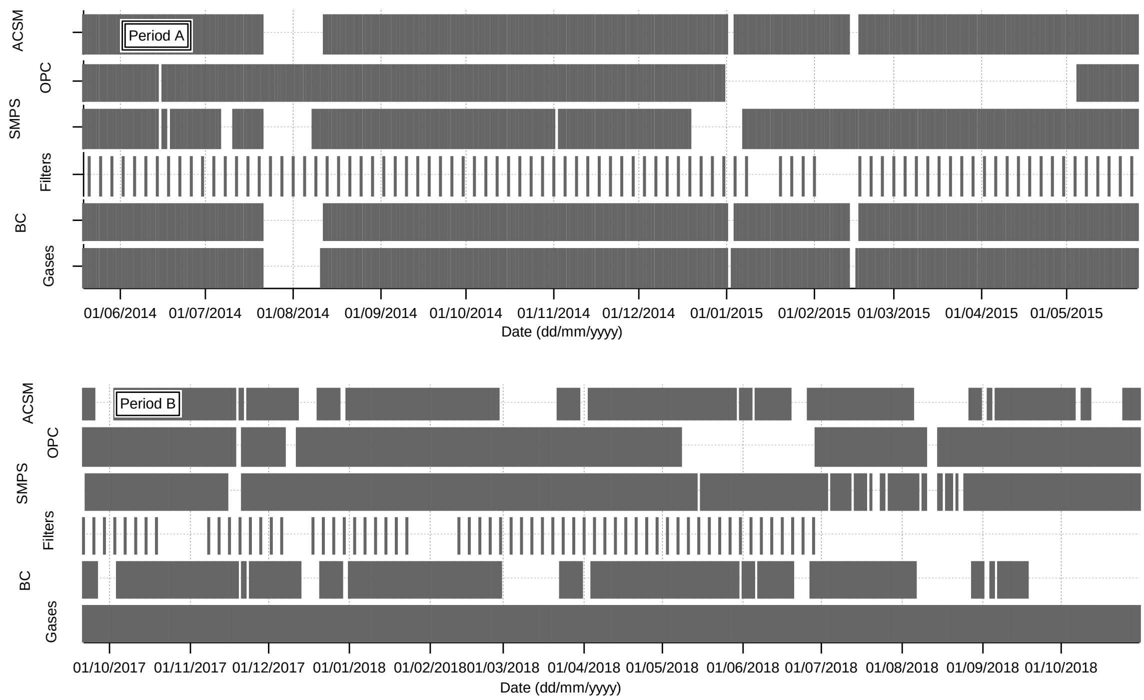

Figure S 2. Data availability for periods A and B.

Table S 1. Output correlations of runs of different number of factors (n) per each season in periods A and B. Bold rows correspond to those selected output runs.

A	n	Q/Qexp	a-value COA	a-value HOA	a-value BBOA	COA vs. m/z55	HOA vs. BC	BBOA vs. m/z60	LO-OOA vs. NO_3^-	MO-OOA vs. SO_4^{2-}	OA meas. vs OA model	
											R^2	Slope
May 2014	3	0.789 ± 0.009	0.3	0.3	-	0.56	0.63	-	0.44	0.04	0.94	1.023±0.011
	4	**0.706 ± 0.008**	**0.5**	**0.1**	**-**	**0.60**	**0.67**	**-**	0.37	**0.21**	0.96	0.996±0.008
	5	0.678 ± 0.011	0.2	0.5	0.1	0.61	0.65	0.28	0.47	0.10	0.98	1.029±0.008
Jun-Aug 2014	3	1.858±0.017	0.1	0.5	-	0.77	0.41	-	0.27	0.12	0.95	1.039±0.004
	4	**1.712±0.004**	**0.1**	**0.5**	**-**	**0.76**	**0.37**	**-**	**0.25**	**0.18**	**0.96**	**1.035±0.004**
	5	1.572±0.017	0.2	0.5	-	0.74	0.34	-	0.23	0.16	0.96	1.025±0.003
Sep-Oct 2014	3	3.188±0.017	0.1	0.5	-	0.66	0.68	-	0.35	0.07	0.95	0.9545±0.0041
	4	**2.929±0.008**	**0.1**	**0.3**	**-**	**0.35**	**0.68**	**-**	**0.35**	**0.08**	**0.96**	**0.968±0.003**
	5	2.76±0.03	0.1	0.5	0.5	0.64	0.68	0.4	0.32	0.09	0.97	0.991±0.004
Nov-Mar 2014-2015	3	9.44±0.05	0.3	05	-	0.68	0.68	-	0.65	0.30	0.97	1.019±0.002
	4	**9.21 ± 0.03**	**0.1**	**0.5**	**0.2**	**0.59**	**0.68**	**0.60**	**0.31**	**0.35**	**0.98**	**1.021±0.002**
	5	8.68 ± 0.07	0.3	0.5	0.1	0.73	0.67	0.60	0.20	0.37	0.98	1.020±0.002
Apr-May 2015	3	4.33±0.09	0.5	0.5	-	0.74	0.45	-	0.40	0.26	0.95	1.023±0.004
	4	**4.10±0.05**	**0.3**	**0.5**	**-**	**0.70**	**0.43**		**0.39**	**0.17**	**0.96**	**1.025±0.004**
	5	3.70±0.05	0.1	0.5	0.3	0.88	0.5	0.4	0.26	0.26	0.96	1.032±0.004
B	**n**	**Q/Qexp**	**a-value COA**	**a-value HOA**	**a-value BBOA**	**COA vs. m/z55**	**HOA vs. BC**	**BBOA vs. m/z60**	**LO-OOA vs. NO_3^-**	**MO-OOA vs. SO_4^{2-}**	**OA meas. Vs. OA app.**	
											R^2	**Slope**
Sep-Oct 2017	3	1.81±0.001	0.1	0.5	-	0.83	0.51	-	0.60	0.15	0.96	1.00 +0.14
	4	**1.053 ± 0.012**	**0.1**	**0.5**	**-**	**0.80**	**0.52**	**-**	**0.59**	**0.33**	**0.96**	**1.01x+0.09**
	5	0.977 ± 0.006	0.1	0.3	0.5	0.61	0.65	0.28	0.53	0.18	0.96	0.96x+0.09
Nov-Mar 2017-2018	4	0.873±0.003	0.3	0.5	0.2	0.68	0.78	0.87	0.80	0.46	0.97	1.013x+0.07
	5	**0.808±0.004**	**0.2**	**0.5**	**0.1**	**0.72**	**0.61**	**0.91**	**0.32**	**0.47**	**0.97**	**1.010x+0.032**
	6	0.765±0.002	0.3	0.5	0.3	0.70	0.78	0.91	0.41	0.47	0.97	1.01x+0.12
Apr-May 2018	3	1.076±0.000	0.1	0.5	-	0.78	0.65	-	0.51	0.18	0.97	1.0x+0.2
	4	**0.893±0.006**	**0.4**	**0.5**	**-**	**0.76**	**0.57**	**-**	**0.42**	**0.32**	**0.97**	**0.90x+0.13**
	5	0.778±0.006	0.3	0.2	0.3	0.69	0.56	0.57	0.42	0.31	0.97	1.00x+0.08
Jun-Aug 2018	3	0.957±0.013	0.5	0.5	-	0.69	0.31	-	0.04	0.05	0.97	1.00x+0.15
	4	**0.869 ± 0.008**	**0.5**	**0.5**	**-**	**0.76**	**0.44**	-	0.1	0.08	0.96	1.00x+0.14
	5	0.809 ± 0.001	0.5	0.4	-	0.76	0.47	-	0.14	0.07	0.96	1.12x+0.15
Sep-Oct 2018	3	1.493±0.008	0.5	0.5	-	0.73	0.74	-	0.25	0.27	0.95	1.02x+0.03
	4	**1.273±0.001**	**0.3**	**0.5**	**-**	**0.74**	**0.74**	**-**	**0.23**	**0.21**	0.97	1.02x-0.02
	5	0.923±0.003	0.3	0.2	0.1	0.73	0.73	0.55	0.17	0.16	0.97	1.03x-0.04

Table S2. Correlations of factors mass spectra with external anchor mass spectra (a), and factors time series with external markers (b).

(a)		Crippa et al., 2013, *Ng et al., 2010				Mohr et al., 2012				
		COA	HOA	BBOA*	OOA	COA	HOA	BBOA	SV-OOA	LV-OOA
A	COA	0.96	0.87	0.74	0.35	0.92	0.76	0.76	0.71	0.19
	HOA	0.77	0.96	0.62	0.34	0.71	0.93	0.62	0.61	0.14
	BBOA	0.25	0.13	0.67	0.36	0.38	0.08	0.35	0.34	0.27
	LO-OOA	0.13	0.06	0.31	0.95	0.27	0.03	0.28	0.66	0.97
	MO-OOA	0.10	0.05	0.25	0.93	0.22	0.02	0.24	‘.65	0.95
B	COA	0.98	0.71	0.66	0.27	0.86	0.58	0.66	0.65	0.16
	HOA	0.79	0.99	0.61	0.19	0.73	0.94	0.65	0.55	0.10
	BBOA	0.62	0.50	0.99	0.40	0.77	0.40	0.72	0.65	0.33
	LO-OOA	0.39	0.25	0.70	0.79	0.64	0.16	0.66	0.75	0.72
	MO-OOA	0.07	0.02	0.03	0.89	0.17	0.05	0.16	0.56	0.94

(b)	Period A	Apr-May 2015	Jun-Aug 2014	Sep - Oct 2014	Nov-Mar 2014-2015	Period B	Ap-May 2018	Jun-Aug 2018	Sep-Oct 2018	Nov-Mar 2017-2018
COA vs. m/z 55	0.58	0.69	0.76	0.35	0.63	0.71	0.76	0.76	0.74	0.72
COA vs. HOA	0.20	0.32	0.24	0.02	0.26	0.31	0.32	0.32	0.28	0.33
HOA vs. BC	0.62	0.42	0.40	0.70	0.63	0.68	0.57	0.57	0.74	0.68
HOA vs. NO	0.44	0.36	0.16	0.53	0.42	0.63	0.41	0.41	0.68	0.76
HOA vs. NO_2	0.49	0.33	0.39	0.51	0.49	0.55	0.51	0.51	0.70	0.75
HOA vs. NO_x	0.44	0.40	0.29	0.45	0.44	0.65	0.51	0.51	0.70	0.75
LO-OOA vs. m/z 43	0.51	0.48	0.25	0.60	-	0.41	0.86	0.86	0.84	0.66
LO-OOA vs. NO_3^-	0.29	0.39	0.74	0.34	-	0.60	0.40	0.68	0.75	0.58
MO-OOA vs. m/z 44	0.60	0.40	0.68	0.75	0.58	0.69	0.84	0.84	0.96	0.96
MO-OOA vs. SO_4^{2-}	0.02	0.09	0.13	0.03	0.03	0.10	0.32	0.32	0.31	0.47
BBOA vs. m/z 60	0.60	-	-	-	0.60	0.91	-	-	-	0.91
BBOA vs. m/z 73	0.55	-	-	-	0.55	0.61	-	-	-	0.61

(a)

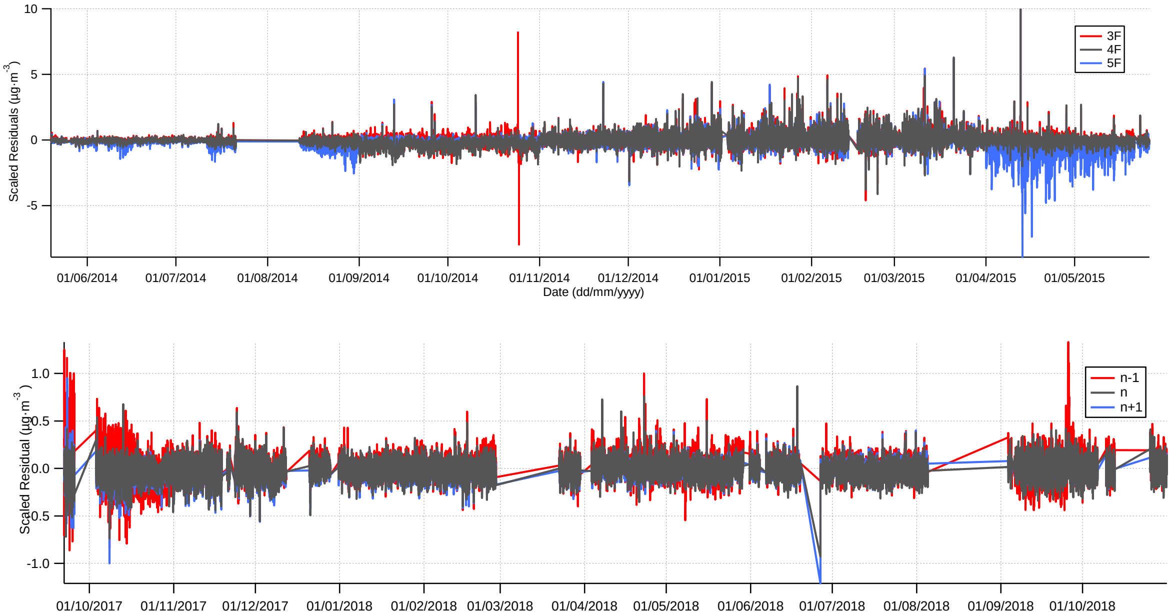

Scaled Residuals (µg·m^{-3})
3F
4F
5F
01/06/2014
01/07/2014
01/08/2014
01/09/2014
01/10/2014
01/11/2014
01/12/2014
01/01/2015
01/02/2015
01/03/2015
01/04/2015
01/05/2015
Date (dd/mm/yyyy)
Scaled Residual (µg·m^{-3})
n-1
n
n+1
01/10/2017
01/11/2017
01/12/2017
01/01/2018
01/02/2018
01/03/2018
01/04/2018
01/05/2018
01/06/2018
01/07/2018
01/08/2018
01/09/2018
01/10/2018

(b)

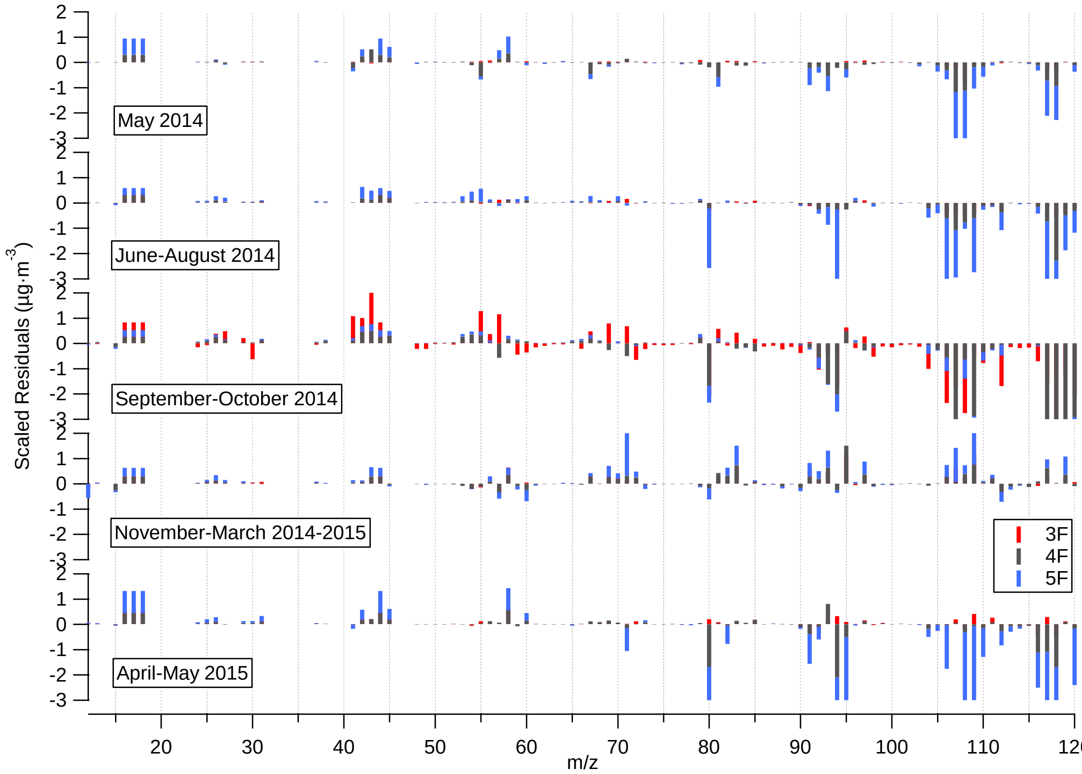

Scaled Residuals (µg·m^{-3})
May 2014
June-August 2014
September-October 2014
November-March 2014-2015
April-May 2015
3F
4F
5F
m/z

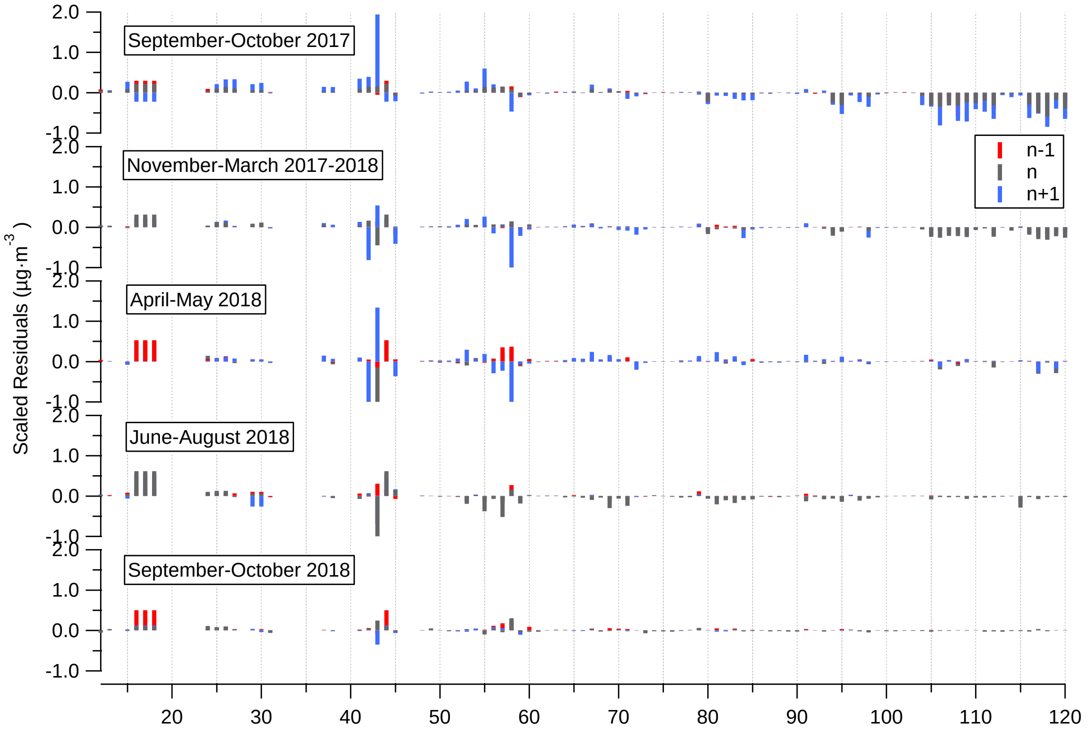

Figure S 3. Scaled residuals (a) time series (b) mass spectra for 3, 4, 5 factors in period A and for n-1, n and n+1 factors in Period B being n the number of factors of the chosen solution.

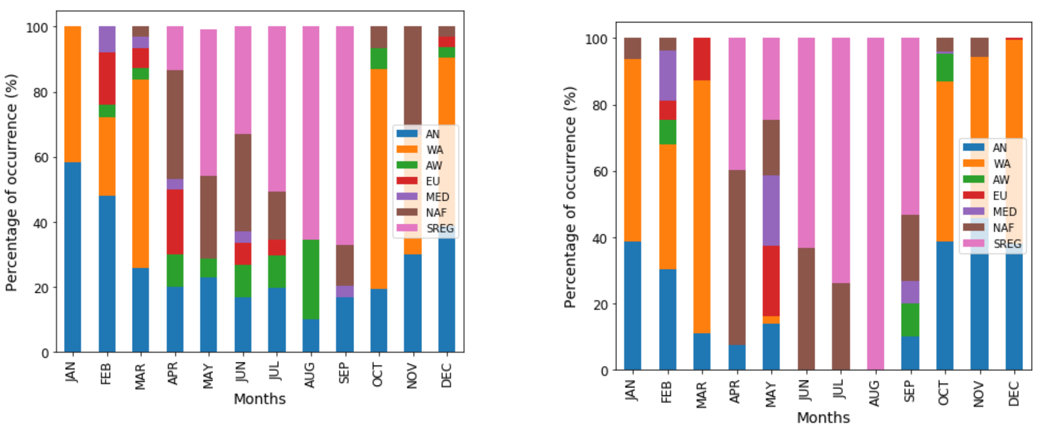

Figure S 4. Relative frequency of occurrence of episodes sorted by month for periods A (left) and B (right).

Table S 3. Comparison between i. total PM_1 from the sum of ACSM components ($NR\text{-}PM_1$) and BC concentrations and co-located measurements of PM_1 from SMPS and ii. ACSM species concentration vs. 24-h samples concentrations. Fit parameters correspond to least orthogonal distance regression method.

(i)		A			B		
y	x	R^2	Slope	Intercept	R^2	Slope	Intercept
$NR\text{-}PM_1$+BC	SMPS (Mass)	0.61	1.001 ± 0.006	0.37 ± 0.07	0.72	1.177 ± 0.006	-0.47± 0.05

(ii)		A			B		
y	x	R^2	Slope	Intercept	R^2	Slope	Intercept
SO_4^{2-} ACSM	SO_4^{2-} off-line	0.88	1.24±0.05	-0.31±0.10	0.93	1.05±0.04	0.01±0.08
NO_3^- ACSM	NO_3- off-line	0.84	1.9±0.1	-0.12±0.09	0.86	1.76±0.09	0.32±0.09
NH_4^+ ACSM	NH4+ off-line	0.85	1.73±0.08	-0.27±0.07	0.71	1.68±0.13	0.05±0.09
OA ACSM	OC off-line	0.73	2.69±0.17	-0.9±0.4	0.86	2.94 ± 0.17	-1.4± 0.3

(a)

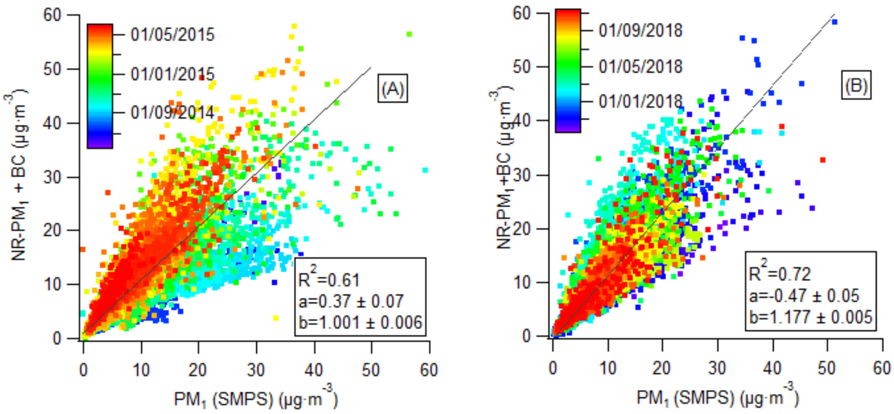

(b)

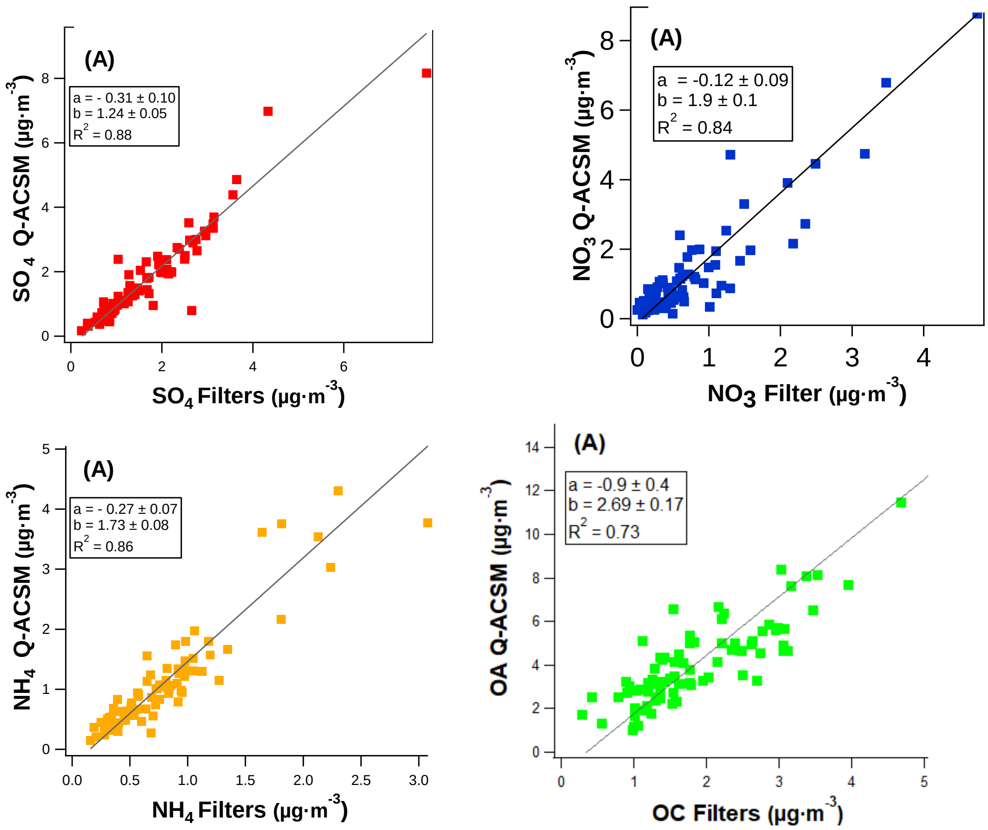

60

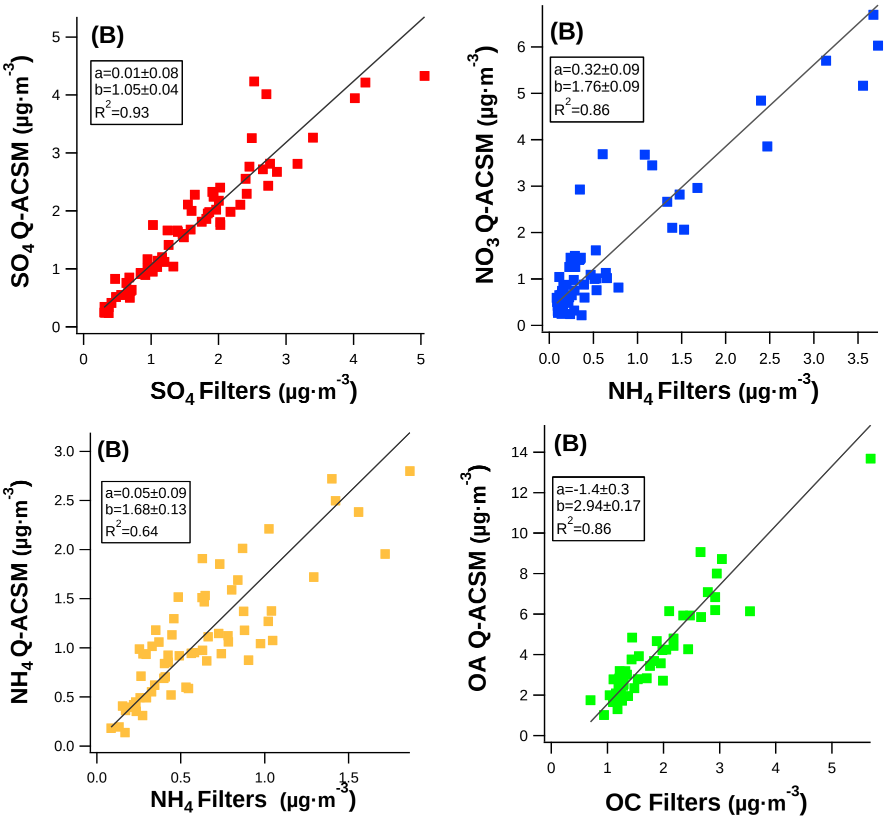

Figure S5. Intercomparison for periods A and B of (a) NR-PM$_1$ from Q-ACSM + BC from MAAP with PM$_1$ measurements from SMPS. (b) NR-PM1 species from Q-ACSM with SO_4^{2-}, NO_3^-, NH_4^+ and OC from filters, respectively.

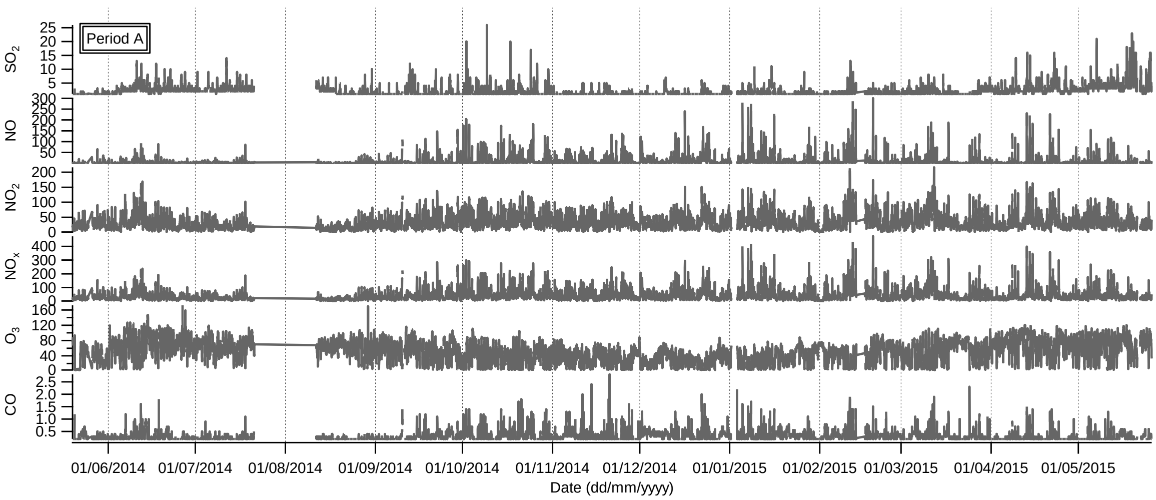

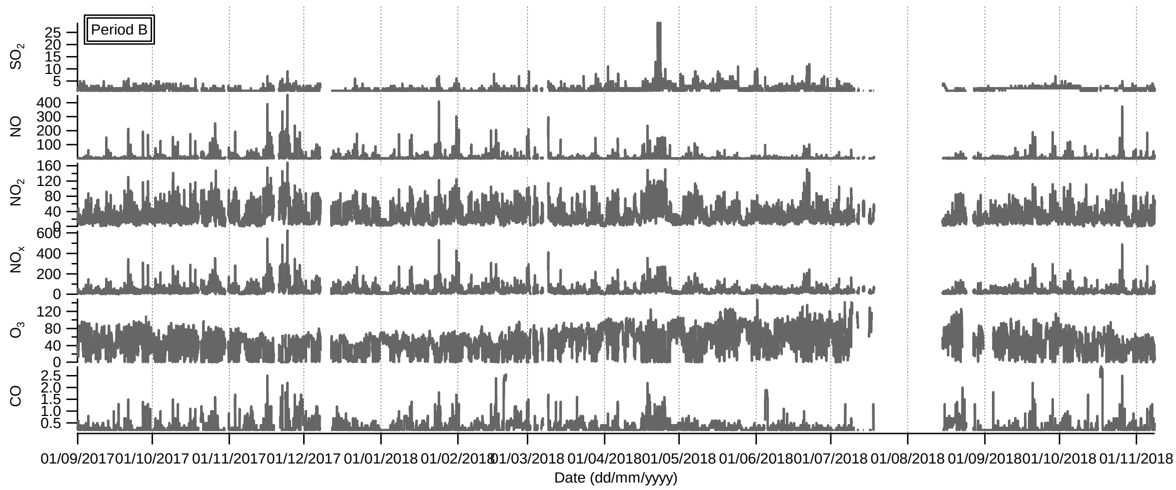

Figure S 6. Time series of co-located gases measurements for period A and B.

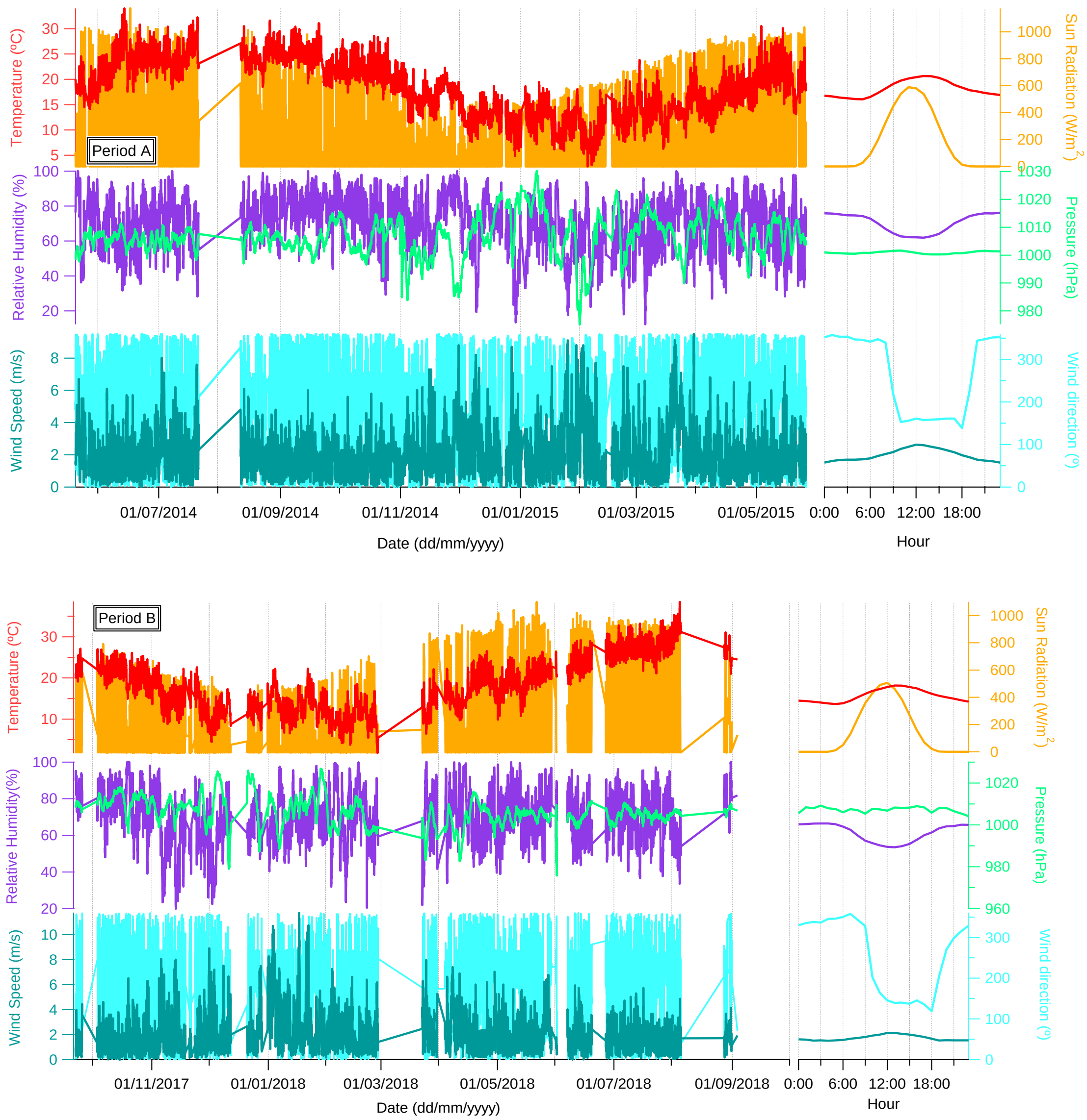

Figure S 7. Time series and diel patterns of meteorological variables for periods A (top) and B (bottom).

Table S4. Period-average mean, standard deviation and percentual change of variables under study for periods A and B.

			Period A		Period B		Change A to B
	Variables	Units	Average	Standard Deviation	Average	Standard Deviation	(%)
Meteorological parameters	Temperature	°C	18.2	5.7	18.4	6.8	+1%
	Relative Humidity	%	70.7	15.3	70.2	14.8	-0.7%
	Pressure	hPa	1006.5	7.3	1005.5	7.32	-0.1%
	Sun Radiation	$W \cdot m^{-2}$	180.0	266.0	178.9	268.5	-0.6%
	Wind Speed	$m \cdot s^{-1}$	2.0	1.4	2.0	1.5	0%
	Wind Direction	°	170.0	102.0	200.4	104.8	+30.4°
Gas-phase pollutants	O_3	$\mu g \cdot m^{-3}$	52.4	28.0	47.6	23.8	- 9%
	CO	$\mu g \cdot m^{-3}$	0.3	0.2	0.3	0.3	0%
	SO_2	$\mu g \cdot m^{-3}$	2.0	1.7	1.7	1.4	-15%
	NO	$\mu g \cdot m^{-3}$	8.3	19.2	8.5	1.2	+2%
	NO_2	$\mu g \cdot m^{-3}$	32.3	24.8	30.6	21.3	-5%
NR-PM_1 ACSM Species	OA	$\mu g \cdot m^{-3}$	4.2	2.8	4.0	2.8	-5%
	SO_4^{2-}	$\mu g \cdot m^{-3}$	1.9	1.5	1.5	1.2	-21%
	NO_3^-	$\mu g \cdot m^{-3}$	1.3	1.7	1.4	1.9	8%
	NH_4^+	$\mu g \cdot m^{-3}$	1.1	0.9	1.0	0.8	-9%
	Cl^-	$\mu g \cdot m^{-3}$	0.05	0.08	0.06	0.08	+20%
MAAP	BC	$\mu g \cdot m^{-3}$	1.7	1.6	1.4	1.4	-18%
ACSM + MAAP	PM_1	$\mu g \cdot m^{-3}$	10.1	6.7	9.6	6.6	-5%
OPC	PM_1	$\mu g \cdot m^{-3}$	8.3	5.4	9.1	5.0	+9%
SMPS	PM_1	$\mu g \cdot m^{-3}$	9.8	7.0	8.5	5.3	-13%
Filters	PM_1	$\mu g \cdot m^{-3}$	8.0	4.2	7.1	3.0	-11%
OA contribution	OA apportioned	$\mu g \cdot m^{-3}$	4.1	2.8	3.8	2.7	-7%
	COA	$\mu g \cdot m^{-3}$	0.7	0.7	0.6	0.5	-14%
	HOA	$\mu g \cdot m^{-3}$	0.8	1.1	0.5	0.8	-37%
	BBOA	$\mu g \cdot m^{-3}$	0.3	0.4	0.2	0.4	-33%
	LO-OOA	$\mu g \cdot m^{-3}$	1.5	1.0	1.1	1.2	-27%
	MO-OOA	$\mu g \cdot m^{-3}$	1.4	1.3	1.7	1.2	21%
	LO-OOA / MO-OOA *	(adim)	1.1	1.6	1.0	1.6	-9%

*** Period-average of the ratio LO-OOA-to-MO-OOA.**

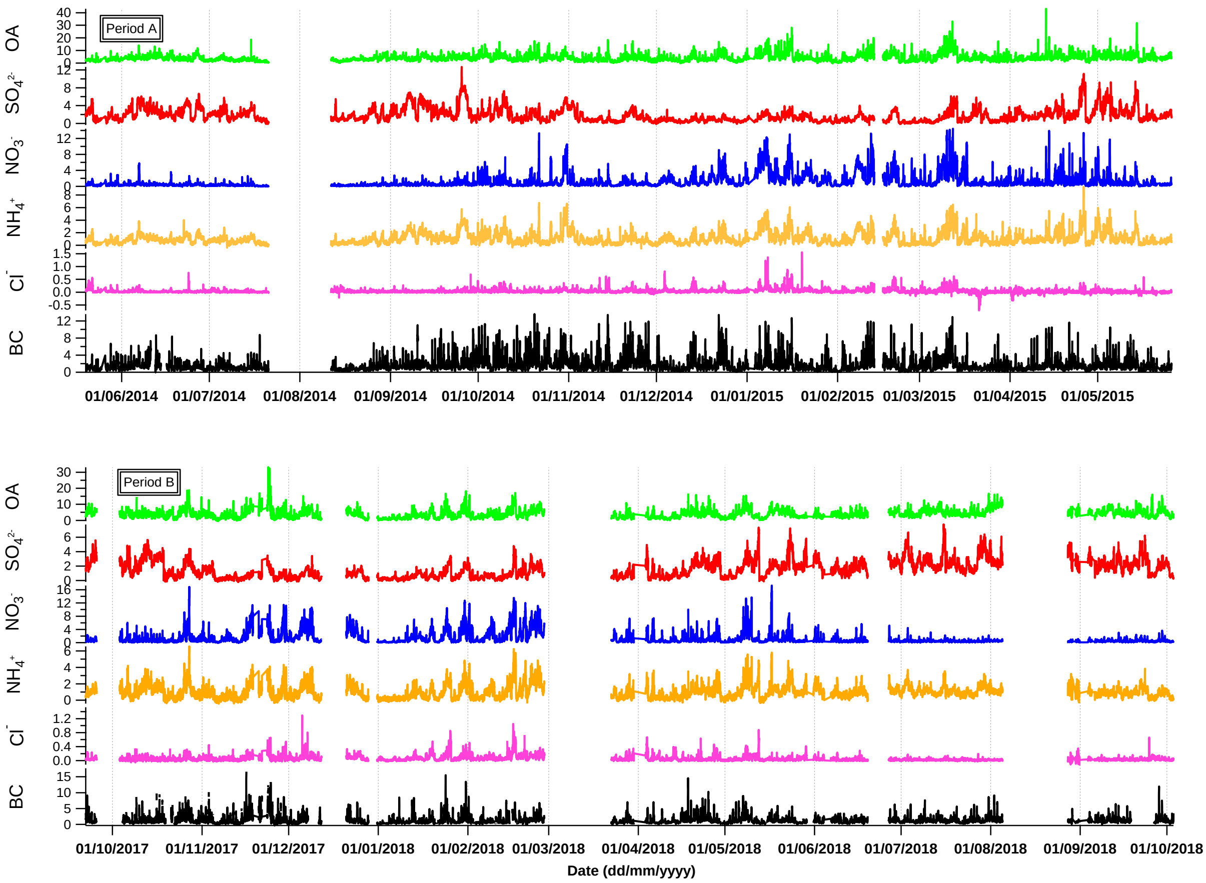

Figure S 8. Time series for NR-PM$_1$ species and BC concentrations in periods A (top) and B (bottom).

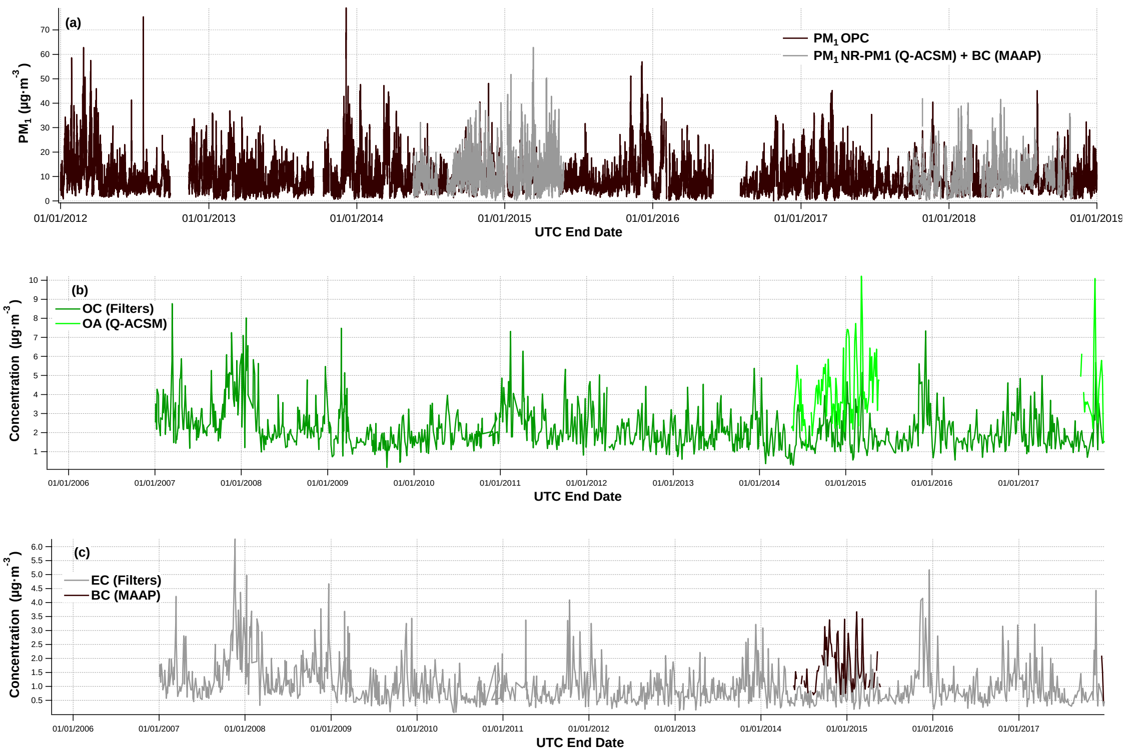

Figure S9. Figure R1. Long-term time series compared to this study two-period time series for respectively, (a) PM1 from OPC and Q-ACSM + MAAP. (b) OC from filters and OM from Q-ACSM. (c) EC from filters and BC from MAAP.

85

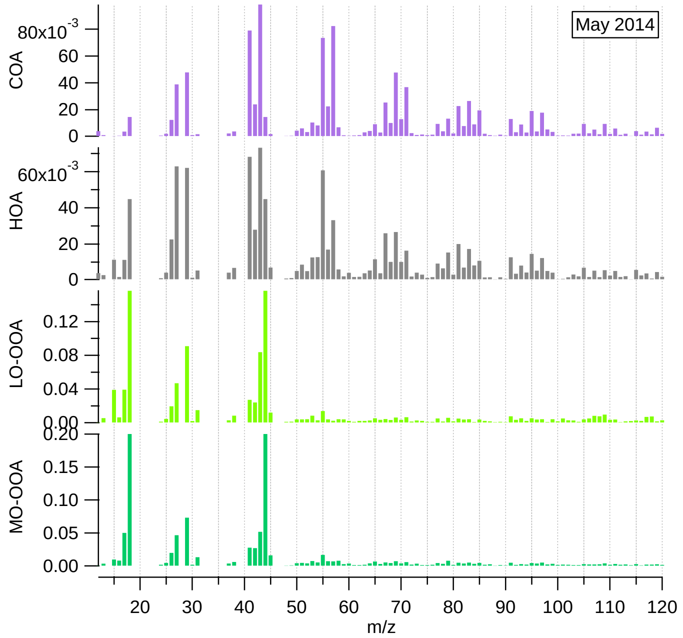
May 2014
COA
HOA
LO-OOA
MO-OOA
m/z

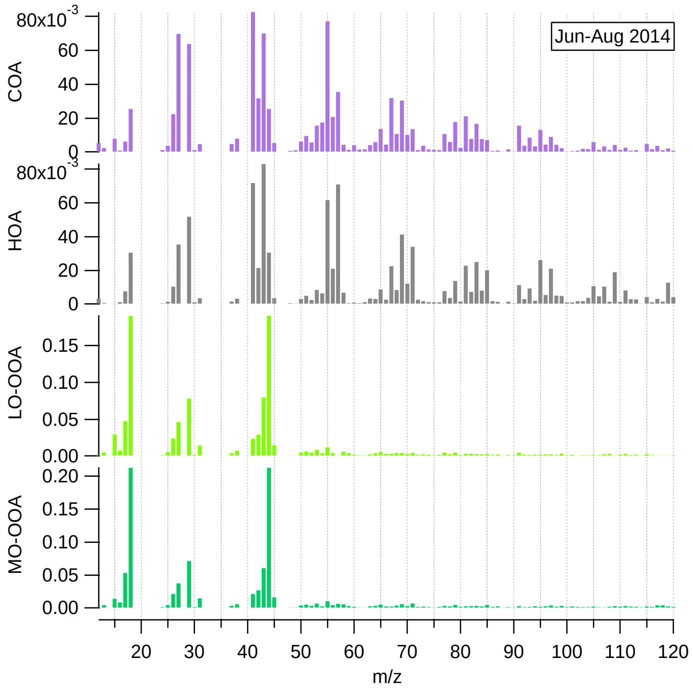
Jun-Aug 2014
COA
HOA
LO-OOA
MO-OOA
m/z

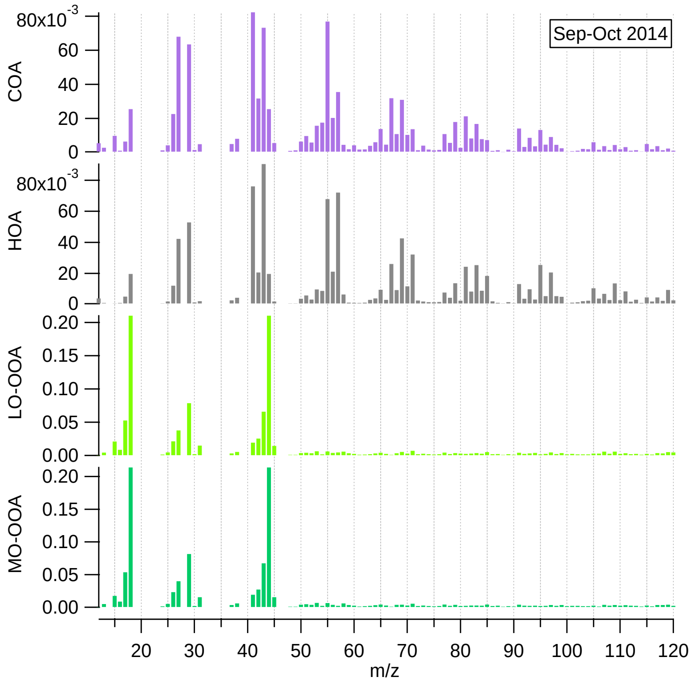
Sep-Oct 2014
COA
HOA
LO-OOA
MO-OOA
80x10^-3
60
40
20
0
0.20
0.15
0.10
0.05
0.00
20 30 40 50 60 70 80 90 100 110 120
m/z

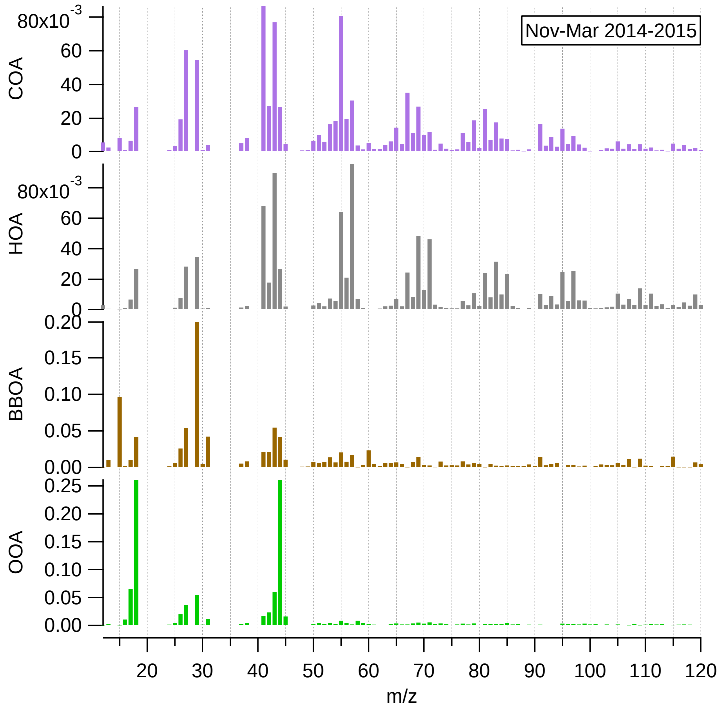
Nov-Mar 2014-2015
COA
HOA
BBOA
OOA
80x10^-3
60
40
20
0
0.25
0.20
0.15
0.10
0.05
0.00
20 30 40 50 60 70 80 90 100 110 120
m/z

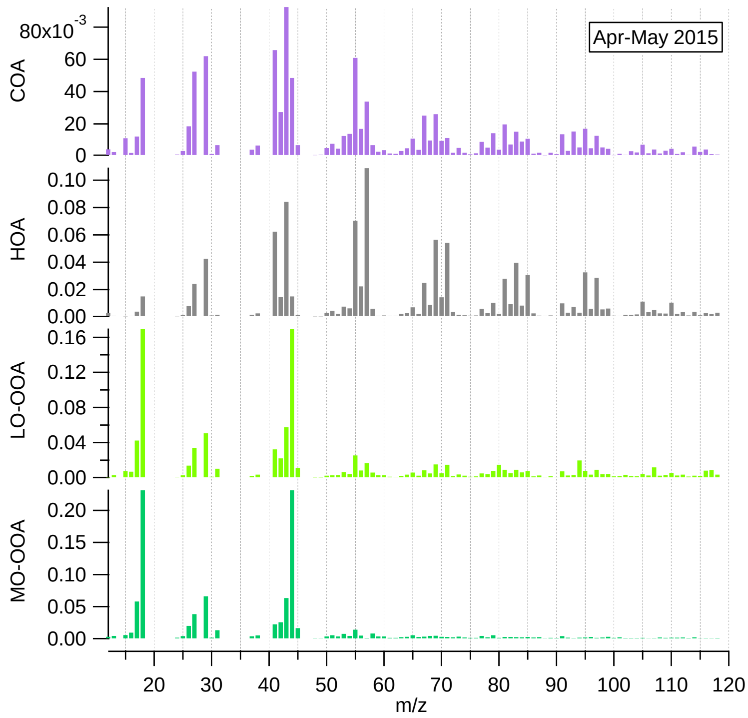
Apr-May 2015
COA
80x10-3
60
40
20
0
HOA
0.10
0.08
0.06
0.04
0.02
0.00
LO-OOA
0.16
0.12
0.08
0.04
0.00
MO-OOA
0.20
0.15
0.10
0.05
0.00
20 30 40 50 60 70 80 90 100 110 120
m/z

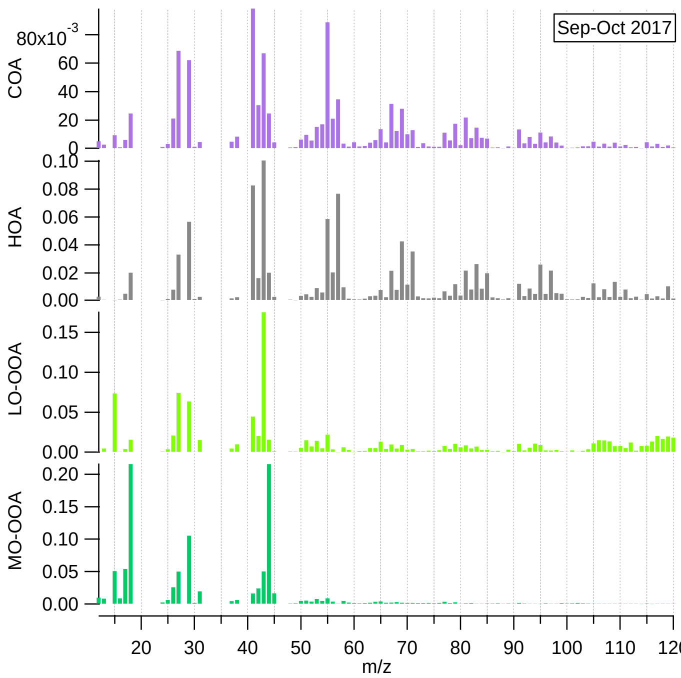
Sep-Oct 2017
COA
80x10-3
60
40
20
0
HOA
0.10
0.08
0.06
0.04
0.02
0.00
LO-OOA
0.15
0.10
0.05
0.00
MO-OOA
0.20
0.15
0.10
0.05
0.00
20 30 40 50 60 70 80 90 100 110 120
m/z

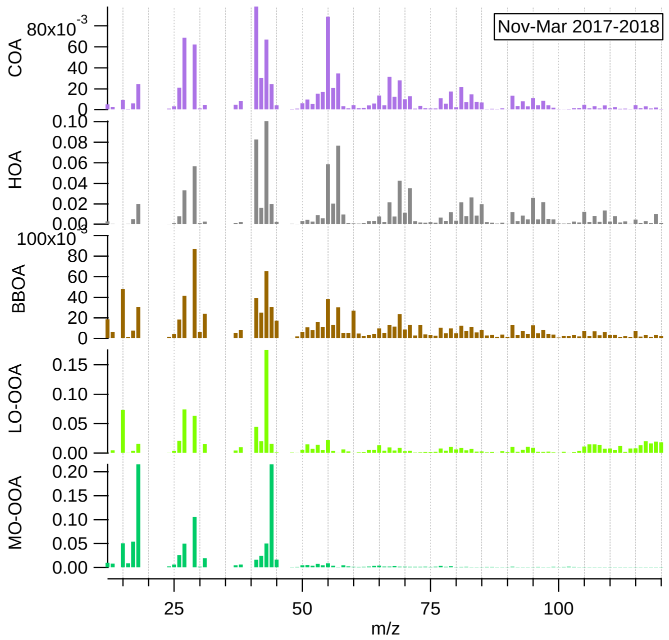
Nov-Mar 2017-2018
COA
HOA
BBOA
LO-OOA
MO-OOA
m/z

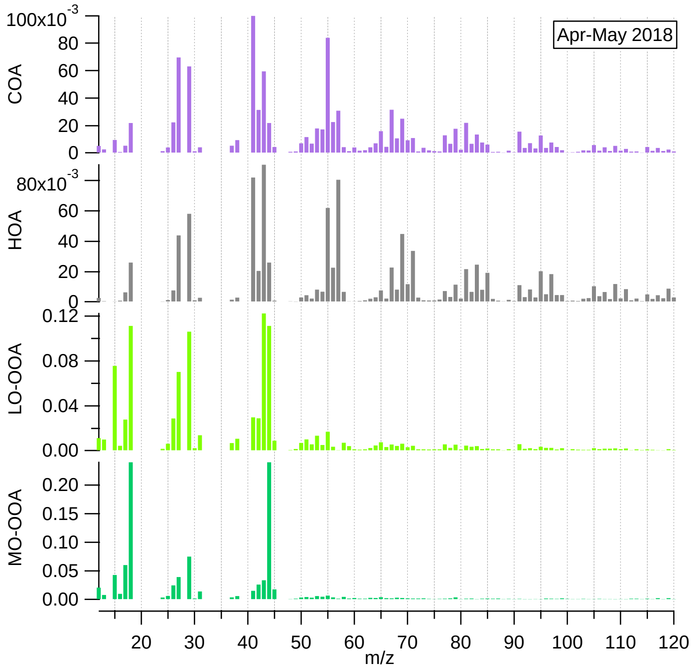
Apr-May 2018
COA
HOA
LO-OOA
MO-OOA
m/z

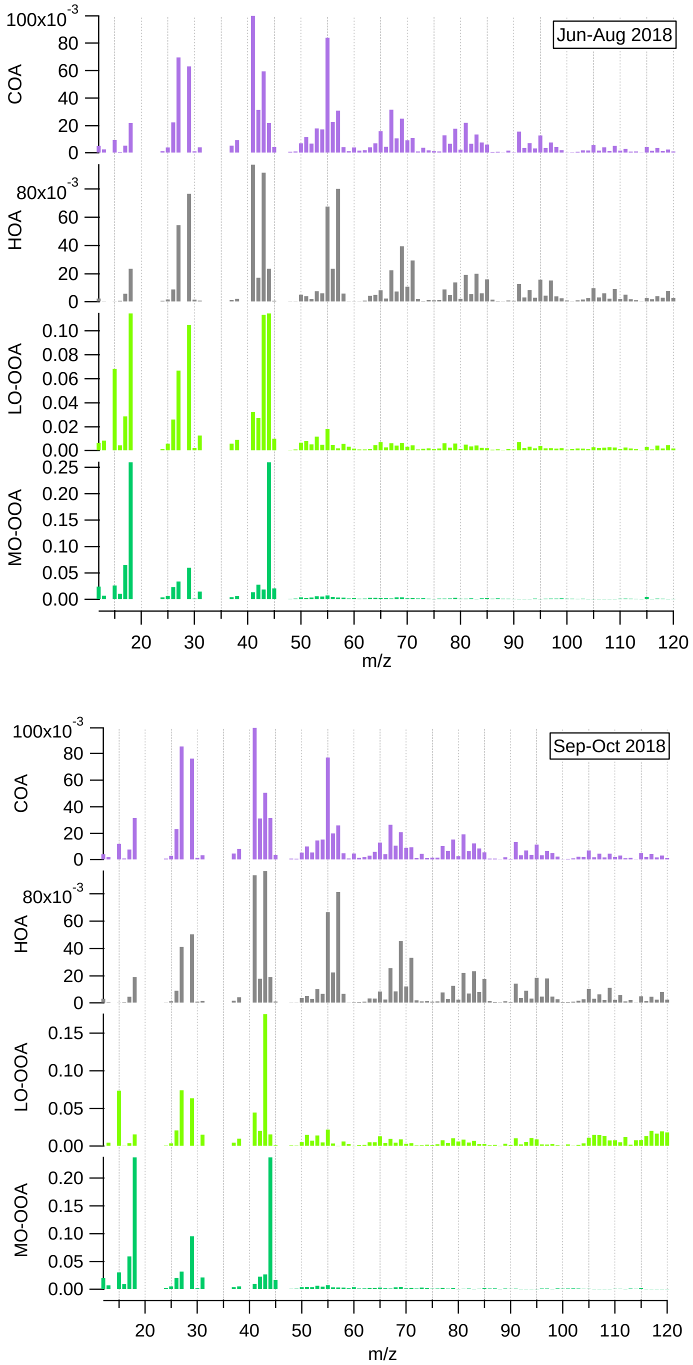

Figure S 10. Seasonal profiles of subperiods of periods A and B by chronological order.

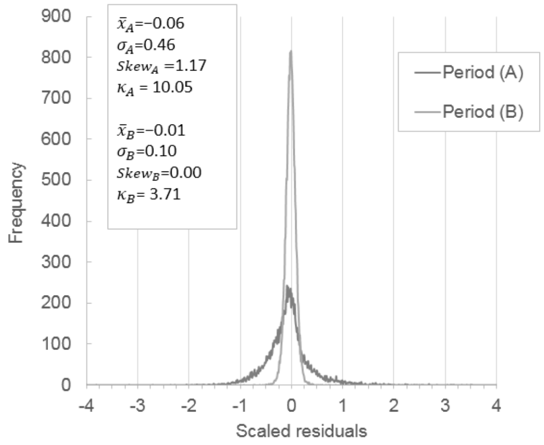

Figure S 11. Residual scaled distributions of PMF OA source distribution using ME-2 approach for periods A and B. Parameters of both distributions (mean, standard deviation and skewness and kurtosis coeffcients) are listed.

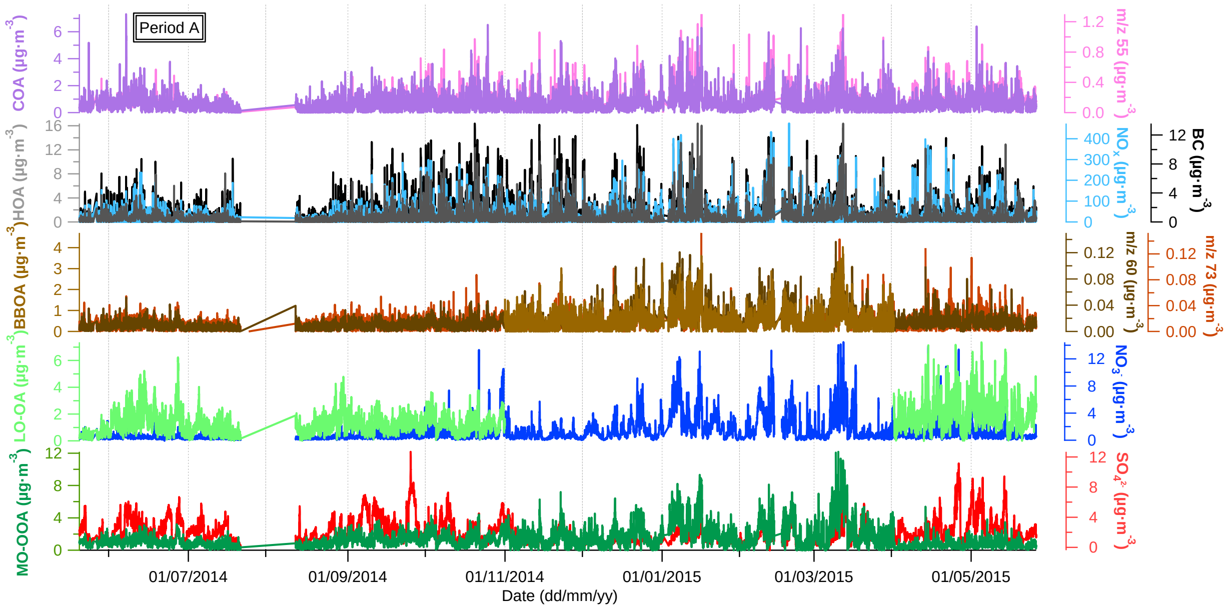

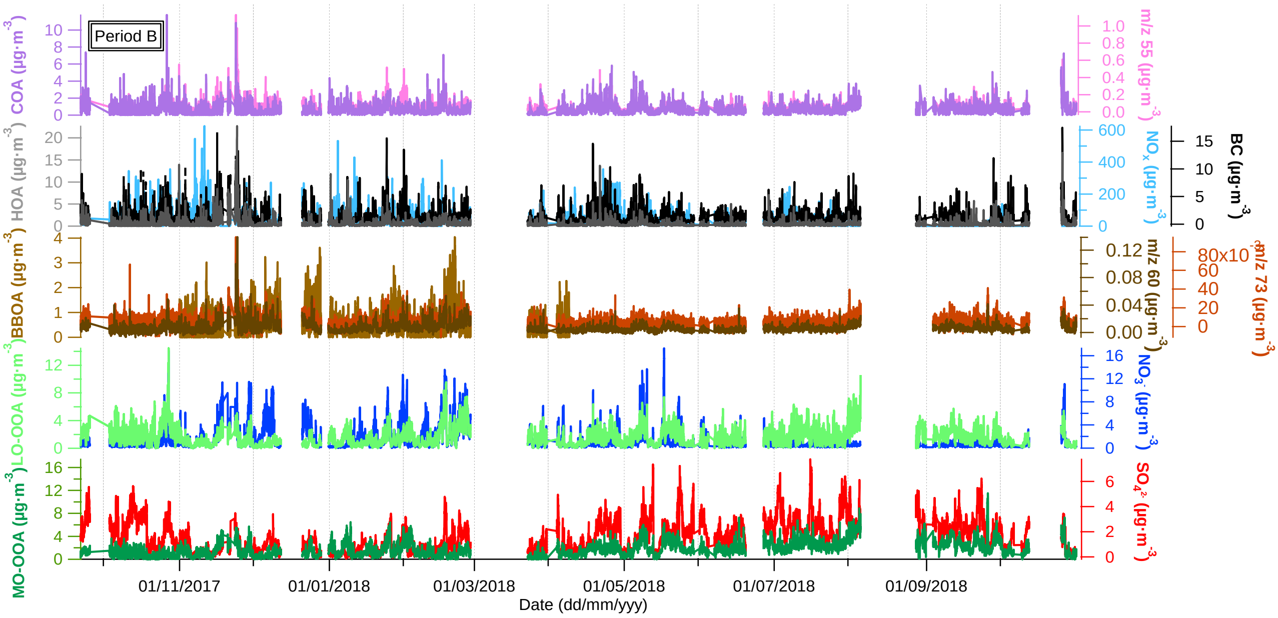

Figure S12. Time series of apportioned OA sources (left axis) and their markers (right axis) in period A and B.

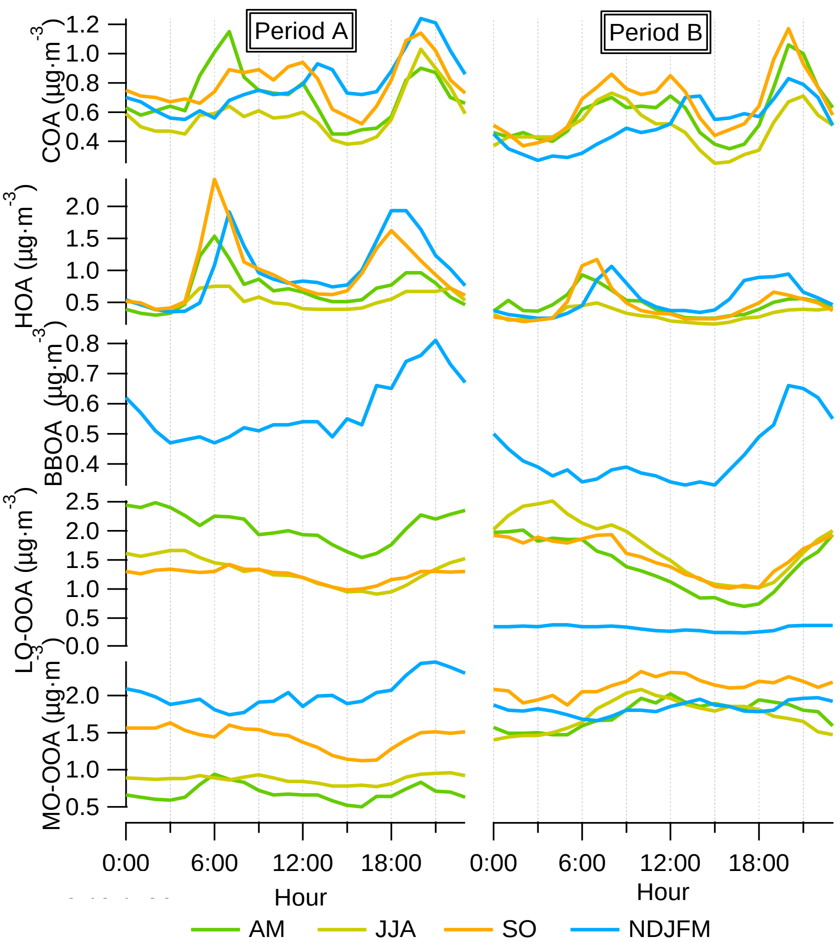

Figure S13. Diel cycle sorted by seasons for the five OA factors for period A and B. Note that the y-axis does not start at zero for the sake of clarity.

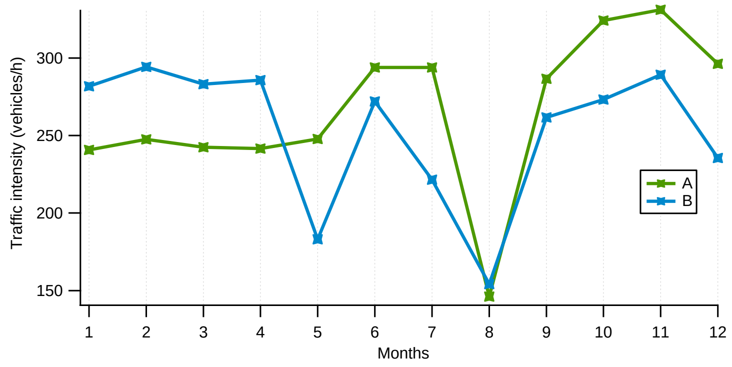

Figure S 14. Mean monthly pattern of traffic intensity at 400m away from site for period A and B.

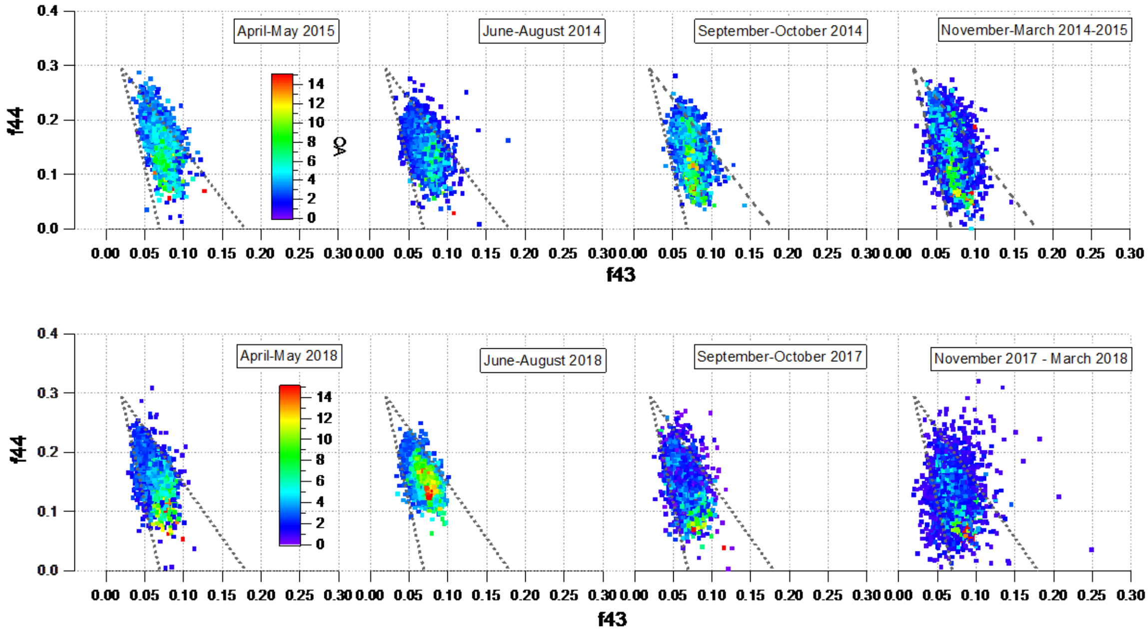

Figure S 15. Seasonal scatterplot of f44 and f43 arranged colored by OA concentrations. Top and bottom graphs correspond to period A and B respectively. Dashed lines correspond to the triangle plot (Ng et al., 2010).

(a)

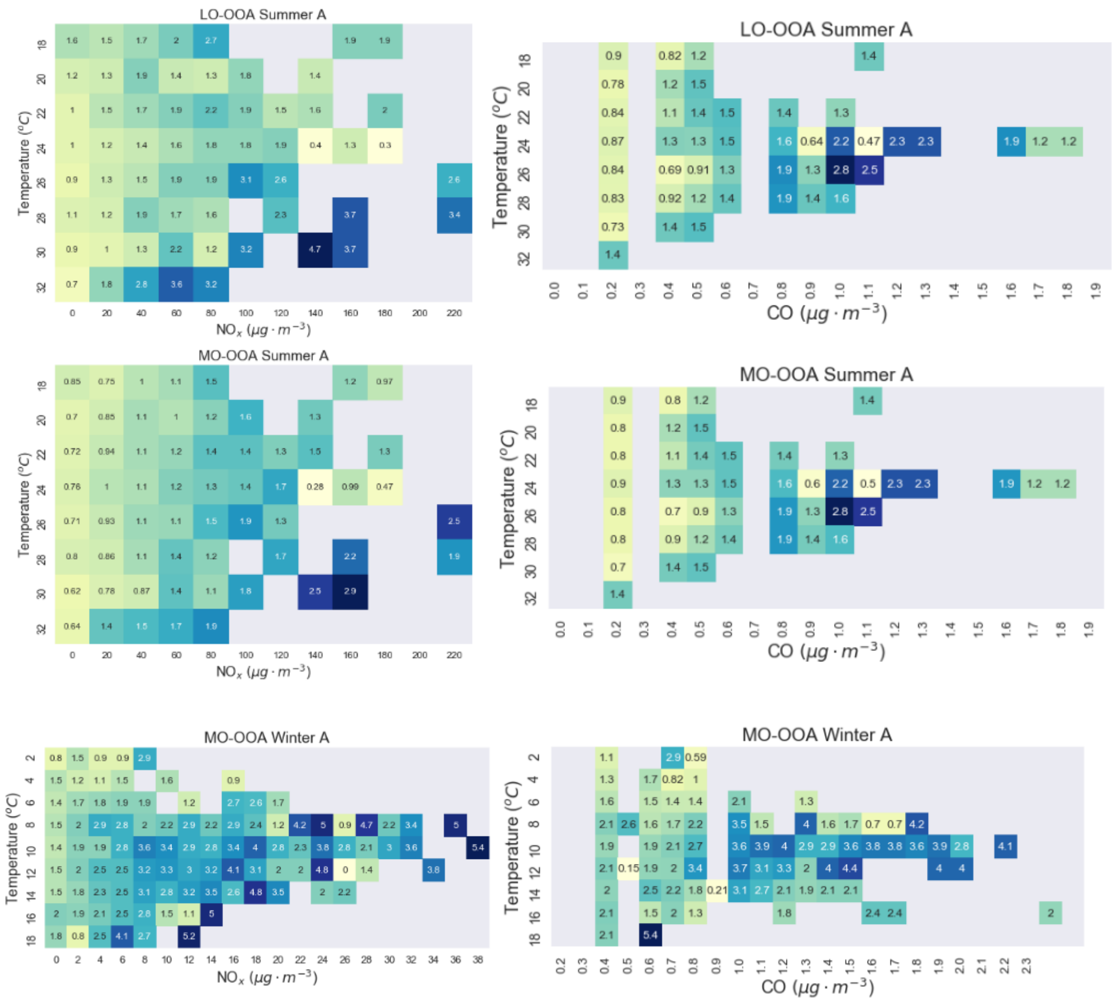
LO-OOA Summer A
Temperature (°C)
NO$_x$ ($\mu g \cdot m^{-3}$)
LO-OOA Summer A
Temperature (°C)
CO ($\mu g \cdot m^{-3}$)
MO-OOA Summer A
Temperature (°C)
NO$_x$ ($\mu g \cdot m^{-3}$)
MO-OOA Summer A
Temperature (°C)
CO ($\mu g \cdot m^{-3}$)
MO-OOA Winter A
Temperature (°C)
NO$_x$ ($\mu g \cdot m^{-3}$)
MO-OOA Winter A
Temperature (°C)
CO ($\mu g \cdot m^{-3}$)

(b)

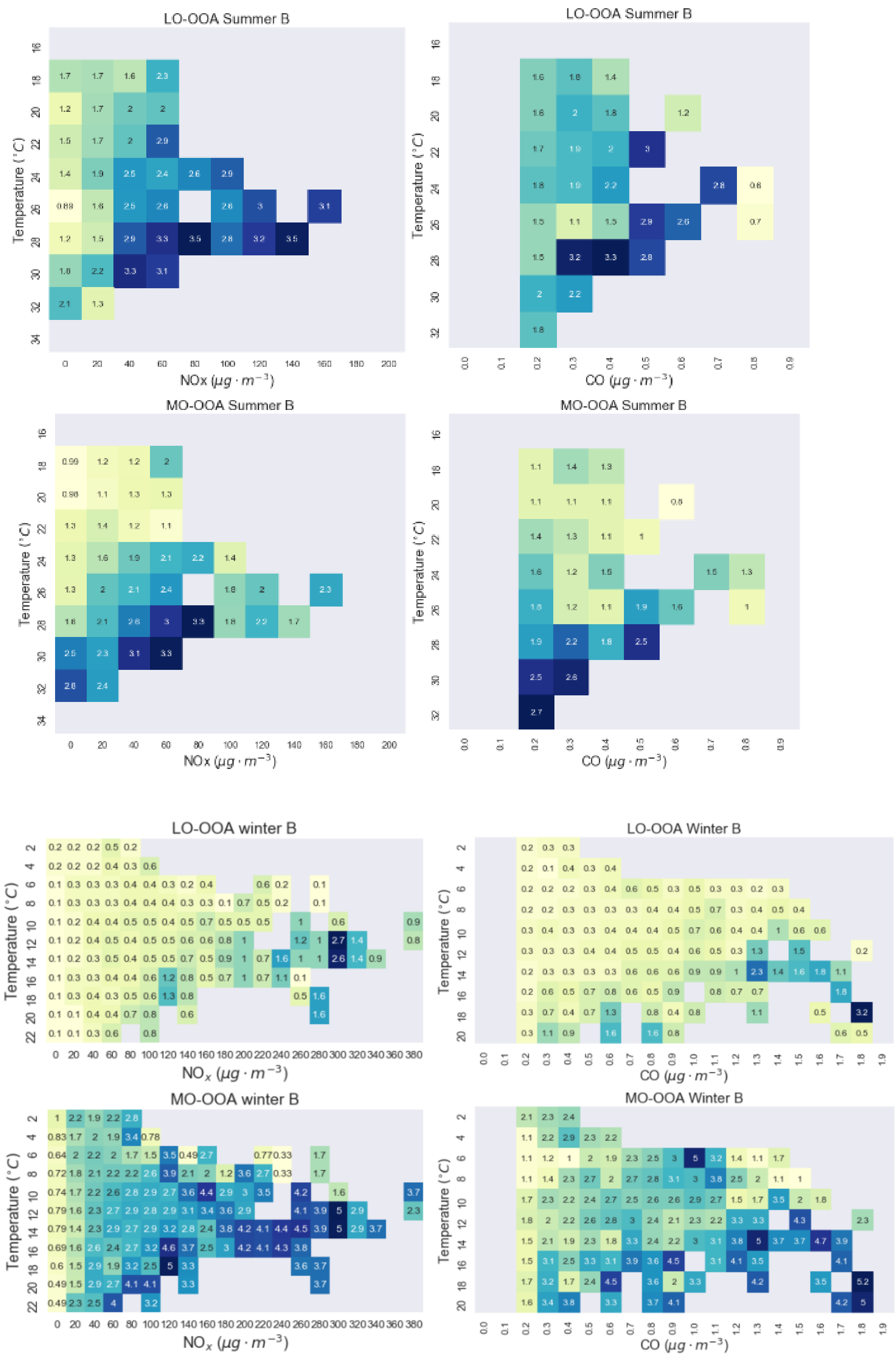

Figure S 16. Heatmap of Temperature vs. NOx for summer (JJA) and winter (DJF) and LO-OOA and MO-OOA respectively for period A (a) and B (b). Figure S 1. Ozone (O_3) diel cycle for seasons in period A (top) and period B (bottom) at Palau Reial (PR) and Montseny (MSY).

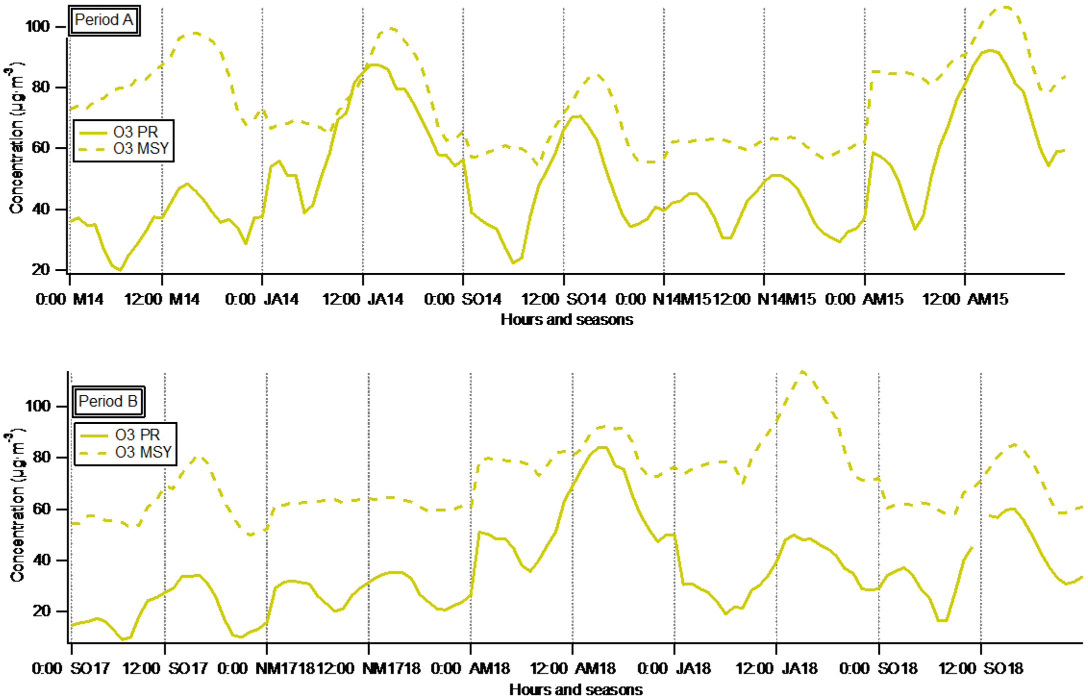

Figure S 17. Ozone diel cycle for seasons in period A and period B at Palau Reial (PR) and Montseny (MSY).

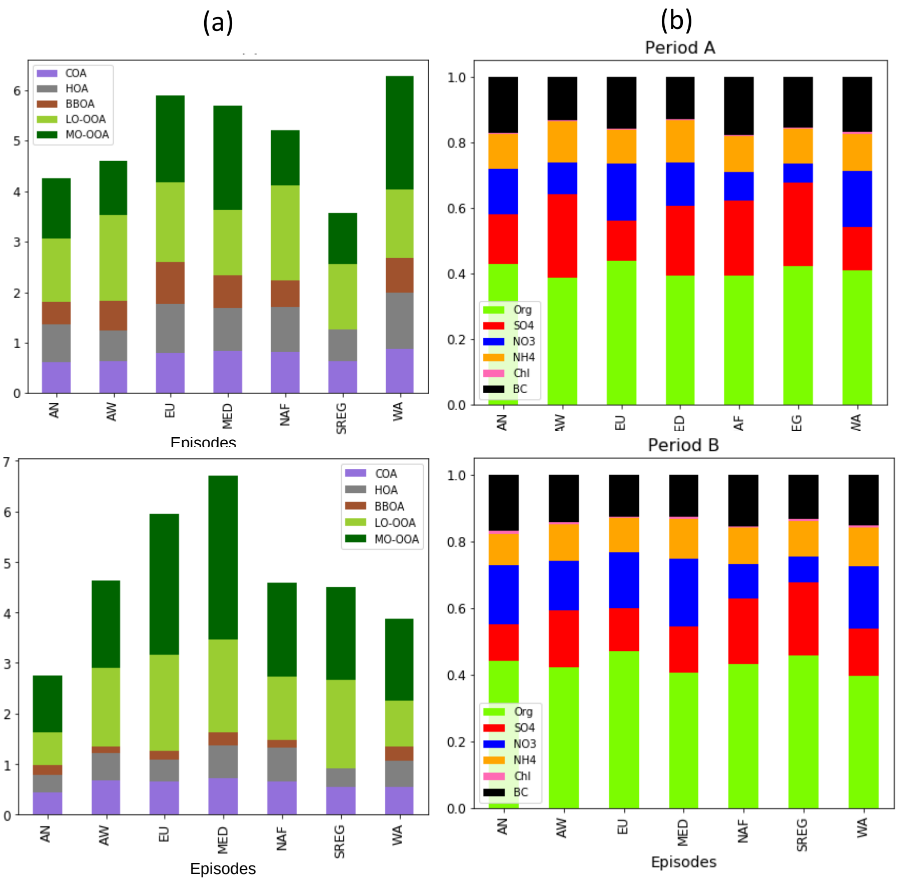

Figure S18. (a) Mean concentrations per each factor grouped by episodes. (c) Relative concentrations of NR-PM1 components grouped by episodes from left to right and for period A (top) and B (bottom).

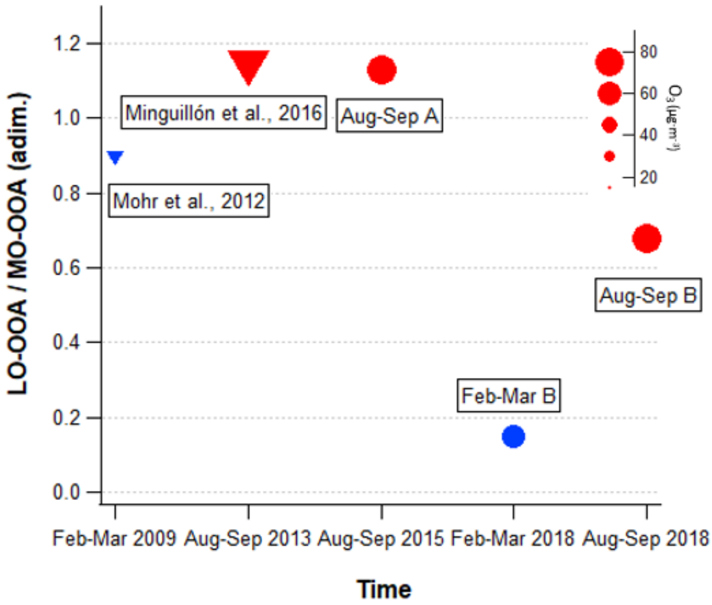

Figure S19. Scatterplot of the LO-OOA-to-MO-OOA ratio vs. time as a function of O3 concentrations (marker size) for the present and previous studies in February-March (blue markers) and August-September (red markers). Note that the Feb-Mar from period A was not included as only one OOA was retrieved.

Section 2. Off-line measurements methodology

PM_1 samples were collected on 150 mm-diameter quartz fiber filters using sequential automatic high-volume samplers Digitel (DHA 80, 30 $m^3 \cdot h^{-1}$). The sampling time was 24 hours midnight to midnight and concentrations were assigned to the start date. Sampling frequency was 1 every 3 days. PM1 levels were determined gravimetrically by conditioning and weighting the filters before and after sampling. Due to problems with the gravimetric determination, PM_1 mass concentration was reconstructed (PM_1 reconstructed) by the addition of all components and an estimation of 25% to account for water.

A complete chemical analysis of the collected PM_1 samples was carried out. A quarter of the filter was used for an acidic digestion (HNO_3:HF:$HClO_4$) following the methodology devised by Querol et al., 2001. The resulting solution was analysed by means of Inductively Coupled Plasma Atomic Emission Spectroscopy (ICP-AES, IRIS Advantage TJA solutions, THERMO) and Inductively Coupled Plasma Mass Spectrometry (ICP-MS, X Series II, THERMO) for the major and trace elements concentration determination, respectively. Few mg of the reference material NIST 1633b were added to a fraction of laboratory blank filters to check the accuracy of the analysis of the acidic digestions.

A quarter of the filter was water extracted and the concentrations of NO_3^- , SO_4^{2-}, and Cl^- were determined by Ion Chromatography (HPLC) using a WATERS ICpakTN anion column with a WATERS 432 conductivity detector. The concentration of NH_4^+ was determined with a Selective Electrode (MODEL 710 A+, THERMO Orion). SO_4^{2-} concentrations in the present study were those calculated from S concentrations determined by ICP-AES, in agreement with all previous works by the research group.

A rectangular portion (1.5 cm^{-2}) of the remaining filter was used for the analysis of organic carbon (OC) and elemental carbon (EC) by thermal-optical methods using a SUNSET OCEC analyser following the EUSAAR 2 protocol (Cavalli et al., 2010).

One blank filter was kept for each set of ten filters. Blank concentrations were subtracted from the total concentration measured for each sample, thus giving ambient concentrations.